THE UNIVERSITY *of* EDINBURGH

Edinburgh Research Explorer

Prospects for a lattice computation of rare kaon decay amplitudes: K +- decays

Prospects for a lattice computation of rare kaon decay amplitudes
$K \to \pi\ell^+\ell^-$ decays

N.H. Christ,[1] X. Feng,[1] A. Portelli,[2] and C.T. Sachrajda[2]

(RBC and UKQCD collaborations)

[1]*Physics Department, Columbia University, New York, NY 10027, USA*

[2]*School of Physics and Astronomy, University of Southampton, Southampton SO17 1BJ, UK*

(Dated: January 29, 2016)

Abstract

The rare kaon decays $K \to \pi\ell^+\ell^-$ and $K \to \pi\nu\bar{\nu}$ are *flavor changing neutral current* (FCNC) processes and hence promising channels with which to probe the limits of the standard model and to look for signs of new physics. In this paper we demonstrate the feasibility of lattice calculations of $K \to \pi\ell^+\ell^-$ decay amplitudes for which long-distance contributions are very significant. We show that the dominant finite-volume corrections (those decreasing as powers of the volume) are negligibly small and that, in the four-flavor theory, no new ultraviolet divergences appear as the electromagnetic current J and the effective weak Hamiltonian H_W approach each other. In addition, we demonstrate that one can remove the unphysical terms which grow exponentially with the range of the integration over the time separation between J and H_W. We will now proceed to exploratory numerical studies with the aim of motivating further experimental measurements of these decays. Our work extends the earlier study by Isidori, Turchetti and Martinelli [1] which focussed largely on the renormalization of ultraviolet divergences. In a companion paper [2] we discuss the evaluation of the long-distance contributions to $K \to \pi\nu\bar{\nu}$ decays; these contributions are expected to be at the level of a few percent for K^+ decays.

I. INTRODUCTION

The rare kaon decays $K \to \pi \ell^+ \ell^-$ and $K \to \pi \nu \bar{\nu}$ are flavor changing neutral current (FCNC) processes which arise in the Standard Model through W-W and γ/Z-exchange diagrams, containing up, charm and top quarks in the loop. As a second-order electroweak interaction, the SM contributions are highly suppressed in FCNC processes, leaving the rare kaon decays as ideal probes for the observation of New Physics effects. Additionally, these decays can be used to determine SM parameters such as V_{td} and V_{ts}, to search for CP violating effects and to test the low-energy structure of QCD as described within the framework of chiral perturbation theory (ChPT). In this paper we discuss the feasibility of computing $K \to \pi \ell^+ \ell^-$ decay amplitudes in lattice simulations; the corresponding study for $K \to \pi \nu \bar{\nu}$ decays will be presented in a forthcoming companion paper [2].

The first observation of 41 $K^+ \to \pi^+ e^+ e^-$ decays was made at the CERN PS accelerator in 1975 [3]. After a long series of experiments spanning 40 years, NA48/2 at the CERN SPS accelerator has observed a sample of 7253 $K^\pm \to \pi^\pm e^+ e^-$ decays [4] and a sample of 3120 $K^\pm \to \pi^\pm \mu^+ \mu^-$ decays [5]. These precision measurements give important information on the low-energy structure of the weak interaction and provide important tests of ChPT. Though expected to be difficult, the first observations of the decays $K_S \to \pi^0 e^+ e^-$ (7 events) [6] and $K_S \to \pi^0 \mu^+ \mu^-$ (6 events) [7] are reported by the NA48/1 experiment at the CERN SPS accelerator. These K_S decays are important in isolating the contribution of direct CP violation in the decay $K_L \to \pi^0 \ell^+ \ell^-$. For these interesting CP-violating K_L decays, upper bounds are set for $\mathrm{Br}(K_L \to \pi^0 e^+ e^-) < 2.8 \times 10^{-10}$ [8] and $\mathrm{Br}(K_L \to \pi^0 \mu^+ \mu^-) < 3.8 \times 10^{-10}$ [9].

On the theoretical side, much work has been done to understand and evaluate both the short- and long-distance contributions to rare kaon decays. Some useful reviews can be found in [10–15]. The CP-conserving decays $K^+ \to \pi^+ \ell^+ \ell^-$ and $K_S \to \pi^0 \ell^+ \ell^-$ are dominated by long-distance hadronic effects induced through the one-photon exchange amplitude. So far the relevant decay amplitudes are studied and parameterized within the framework of ChPT [16, 17]. A challenge, but also an opportunity, for the lattice QCD community is to compute the decay amplitudes reliably, as well as determining the necessary low-energy constants used in ChPT. We will explain in the following section that the significant interference between the direct and indirect CP violating components of the decay $K_L \to$

$\pi^0 \ell^+ \ell^-$ (see Refs. [18, 19]) implies that lattice QCD results for K_S decays can be used to evaluate the CP-violating contributions to K_L decays. In Ref. [1] it had already been proposed to calculate the long-distance contributions to rare kaon decays using lattice QCD. Our work builds on Ref. [1] and leads us to conclude that such computations are feasible with present understanding and recent theoretical and technical advances.

The remainder of this paper is organized as follows. In the next section we review the phenomenological background for $K \to \pi \ell^+ \ell^-$ decays with an emphasis on the long-distance contributions. The procedure to obtain the amplitudes from lattice simulations is presented in Sec. III. Finite-volume effects and renormalization are briefly discussed in Sec. IV and V respectively. Finally we present our conclusions in Sec. VI.

II. PHENOMENOLOGICAL BACKGROUND

In $K \to \pi \ell^+ \ell^-$ decays, the loop function associated with the γ-exchange diagrams has a logarithmic dependence on the masses of the quarks entering in the FCNC process (this is known as logarithmic or soft Glashow, Iliopoulos, Maiani (GIM) mechanism). The un-suppressed sensitivity to the light-quark mass is a signal of long-distance dominance in the CP-conserving $K^+ \to \pi^+ \ell^+ \ell^-$ and $K_S \to \pi^0 \ell^+ \ell^-$ decays. The short-distance contribution to the amplitude from Z-exchange and W-W diagrams also exists, but is much smaller than the long-distance part induced by the γ-exchange diagrams and does not play an important role in the total branching ratio. This logarithmic GIM mechanism does not apply to direct CP violation in $K_L \to \pi^0 \ell^+ \ell^-$ decays since $\mathrm{Im}\,\lambda_u = 0$ where $\lambda_q = V_{qs}^* V_{qd}$. As a result, the direct CP-violating contribution is short-distance dominated.

Considering only the dominant one-photon exchange contribution, the amplitude A_i ($i = +, S$) for K^+ and K_S decays can be written in terms of an electromagnetic transition form factor $V(z)$ [17, 20]

$$A_i = -\frac{G_F \alpha}{4\pi} V_i(z)(k+p)^\mu \, \overline{u}_\ell(p_-)\gamma_\mu v_\ell(p_+) \,, \tag{1}$$

where $z = q^2/M_K^2$ and $q = k - p$. Here we follow the notation used in Ref. [15]; k, p and $p_\pm$ indicate the momenta of the K, π and $\ell^\pm$, respectively. For both K^+ and K_S decays, the form factor $V_i(z)$ has been analyzed in ChPT [17] and has been parameterized in the form

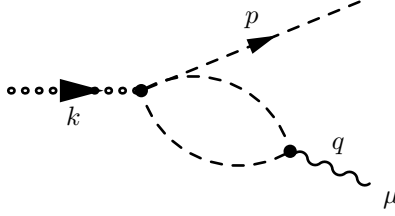$$V_i(z) = a_i + b_i z + V_i^{\pi\pi}(z) \,. \tag{2}$$

3

Figure 1. One-loop contribution in ChPT to the decays $K_S \to \pi^0 \ell^+ \ell^-$ and $K^+ \to \pi^+ \ell^+ \ell^-$. The dashed, circled and wiggly lines represent the pions, kaon and photon respectively. There is a branch cut when $q^2 > 4M_\pi^2$.

Here $V_i(z)$ is analytic in the complex z-plane, with a branch cut starting from $4r_\pi^2$, where $r_\pi = M_\pi/M_K$. As shown in Fig. 1, at low energies the $\pi\pi$ intermediate state is expected to play the dominate role. Thus $V_i^{\pi\pi}(z)$ is introduced to take account of the $\gamma^* \to \pi\pi$ effects. The contribution of excited intermediate states is not given explicitly and may be accounted for by the assumed polynomial correction $a_i + b_i z$. A detailed expression for $V_i^{\pi\pi}(z)$ is given in [17]. As a standard twice-subtracted dispersion relation, $V_i^{\pi\pi}(z)$ satisfies $V_i^{\pi\pi}(0) = 0$. Therefore, the inclusion of $V_i^{\pi\pi}(z)$ does not affect a_i, which is the form factor $V_i(z)$ at zero momentum transfer. The a_i and b_i, can be determined using the experimental data using the dilepton invariant mass spectra as inputs. The parameterization (2) provides a successful description of the $K^+ \to \pi^+ \ell^+ \ell^-$ data but shows large corrections beyond leading order in ChPT [17]. A lattice QCD calculation can help to understand the origin of these large corrections.

For K_S decays, only a few events have been observed in experiments. The dilepton invariant–mass spectra are therefore unavailable. Assuming vector meson dominance, the authors of [17] used the branching ratios to determine the parameter $|a_S|$ and obtain $|a_S| = 1.06^{+0.26}_{-0.21}$ for the electron and $|a_S| = 1.54^{+0.40}_{-0.32}$ for the muon. There are two drawbacks of using the branching ratios: they do not give information about the explicit z-dependence and only the modulus of a_S can be determined. It would be very useful if lattice QCD calculations could determine the sign of a_S and also provide a test for the vector meson dominance assumption.

$K_L \to \pi^0 \ell^+ \ell^-$ decays are interesting for precision studies of CP violation. The relevant decay amplitudes receive three major contributions [18, 19]:

1. a short-distance dominated direct CP-violating term, see Fig. 2(a1,a2),
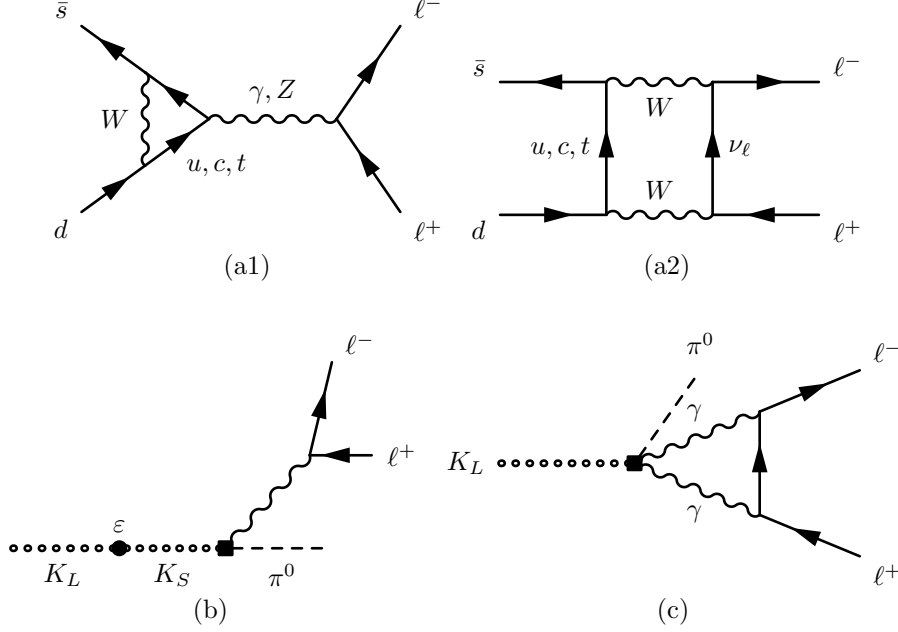
4

Figure 2. The three major contributions to $K_L \to \pi^0\ell^+\ell^-$ decays: (a1,a2) short-distance dominated penguin and box diagrams, (b) long-distance dominated indirect CP violating contribution occurring through $K^0 - \overline{K}^0$ mixing, (c) long-distance dominated CP conserving component involving two-photon exchange.

2. a long-distance dominated indirect CP-violating contribution from the decay of the CP-even component of K_L ($K_1 \simeq K_S$), see Fig. 2(b),

3. a CP-conserving component which proceeds through two-photon exchanges, see Fig. 2(c).

These three contributions are of comparable size [18]. Here we mainly focus on the CP violating effects. The total CP-violating contributions to the K_L branching ratios are summarized in [15] as

$$\text{Br}(K_L \to \pi^0 e^+ e^-)_{\text{CPV}} = 10^{-12} \times \left[15.7|a_S|^2 \pm 6.2|a_S| \left(\frac{\text{Im}\,\lambda_t}{10^{-4}} \right) + 2.4 \left(\frac{\text{Im}\,\lambda_t}{10^{-4}} \right)^2 \right] \qquad (3)$$

$$\text{Br}(K_L \to \pi^0 \mu^+ \mu^-)_{\text{CPV}} = 10^{-12} \times \left[3.7|a_S|^2 \pm 1.6|a_S| \left(\frac{\text{Im}\,\lambda_t}{10^{-4}} \right) + 1.0 \left(\frac{\text{Im}\,\lambda_t}{10^{-4}} \right)^2 \right], \qquad (4)$$

where the $|a_S|^2$-term comes from the indirect CP-violating component of the amplitude, the $(\text{Im}\,\lambda_t)^2$-term comes from the direct CP-violating component and the $|a_S|(\text{Im}\,\lambda_t)$-terms are the interference between the indirect and direct components. The $\pm$ symbol indicates that

5

the sign of a_S is unknown. $|a_S|$ are quantities which are expected to be of $O(1)$ and the CKM matrix element takes the value $\text{Im}\,\lambda_t/10^{-4} \approx 1.34$. A change in the sign of a_S can cause a large difference in the predicted branching ratios for both $K_L \to \pi^0 e^+ e^-$ and $K_L \to \pi^0 \mu^+ \mu^-$ decays. Once lattice QCD has determined the sign of a_S, this large uncertainty will be clarified.

In this paper we do not address the evaluation of the CP-conserving (CPC) component of the $K_L \to \pi^0 \ell^+ \ell^-$ amplitude given by the two-photon exchange diagram in Fig. 2(c). The helicity suppression of the angular momentum $J = 0$ channel leads to a negligible contribution (of $O(10^{-14})$ to the branching ratio) for the electron mode, but a comparable contribution to the CP-violating one for the muon mode. For example, using a phenomenological study based on ChPT, the authors of Ref. [18] estimate

$$\text{Br}(K_L \to \pi^0 \mu^+ \mu^-)_{\text{CPC}} = (5.2 \pm 1.6)\ 10^{-12}\,. \tag{5}$$

The $J = 2$ contribution on the other hand is expected to be negligible for the muon channel, but may be of $O(10^{-13})$ for the electron channel so that the decay $K_L \to \pi^0 e^+ e^-$ is predominantly CP-violating [15]. Nevertheless, in due course after we manage to compute the $K_L \to \pi^0 \gamma^* \to \pi^0 \ell^+ \ell^-$ contribution to the decay amplitude, it will be an interesting challenge to compute the two-photon exchange contribution.

Since the phenomenology of rare kaon decays has, up to now, been based on ChPT much of the discussion of this section has been in this context. We stress however, that the goal of lattice computations reaches beyond the evaluation of the low energy constants. The amplitudes will be calculated from first principles at several values of q^2 and the results themselves can then be used in future phenomenological studies.

III. EVALUATION OF THE AMPLITUDES IN EUCLIDEAN SPACE-TIME

In this section we discuss the evaluation of rare kaon decay amplitudes using lattice computations of Euclidean correlation functions. We start however, with the definition and a discussion of the amplitudes in Minkowski space.

A. Definition of the amplitude

The long distance part of the $K^+ \to \pi^+ \ell^+ \ell^-$ and $K^0 \to \pi^0 \ell^+ \ell^-$ decay amplitudes is given by [17, 20]:

$$\mathcal{A}^j_\mu(q^2) = \int d^4x \, \langle \pi^j(\mathbf{p})| \, T[J_\mu(0) H_W(x)] \, |K^j(\mathbf{k})\rangle \, . \tag{6}$$

The external states are on their mass shells and we define $q \equiv k - p$. The index $j = +, 0$ labels the charge of the mesons, and H_W is the effective weak Hamiltonian density defined by [1]:

$$H_W(x) = \frac{G_F}{\sqrt{2}} V^*_{us} V_{ud} \left[C_1(Q^u_1 - Q^c_1) + C_2(Q^u_2 - Q^c_2) \right], \tag{7}$$

where the C_i are the Wilson coefficients in a chosen renormalization scheme. $Q^q_{1,2}$ are the following current-current local operators:

$$Q^q_1 = (\bar{s}_a \gamma^L_\mu d_a)(\bar{q}_b \gamma^{L\,\mu} q_b) \qquad \text{and} \qquad Q^q_2 = (\bar{s}_a \gamma^L_\mu q_a)(\bar{q}_b \gamma^{L\,\mu} d_b) \, , \tag{8}$$

where a and b are summed color indices and $\gamma^L_\mu = \gamma_\mu(1 - \gamma_5)$. We envisage working in the four-flavor theory and exploiting the GIM cancellation of ultraviolet divergences as explained in Sec. V. The electromagnetic current J_μ is the standard flavor-diagonal vector current:

$$J_\mu = \frac{1}{3}(2V^u_\mu - V^d_\mu + 2V^c_\mu - V^s_\mu) \, . \tag{9}$$

Electromagnetic gauge invariance implies that each non-local matrix element can be written in terms of a single invariant form factor:

$$\int d^4x \, \langle \pi^j(\mathbf{p})| \, T[J_\mu(0)(Q^u_i(x) - Q^c_i(x))] \, |K^j(\mathbf{k})\rangle \equiv \frac{w^j_i(q^2)}{4\pi^2} \left[q^2(k+p)_\mu - (M^2_K - M^2_\pi)q_\mu \right] \tag{10}$$

and the non-perturbative QCD effects are contained in the form factors $w^j_i(q^2)$. In the phenomenological studies described in Sec. II, the $w^j_i(q^2)$ are written in terms of a parametrization influenced by ChPT. Note that a consequence of (10) is that the matrix elements vanish when $\mathbf{p} = \mathbf{k} = 0$, i.e. when the invariant mass of the lepton pair is the largest which is kinematically allowed, $q^2 = q^2_{\max}$. Thus to obtain non-zero matrix elements at least one of the mesons must have a non-zero three-momentum.

Inserting a complete set of states in each of the two possible time-orderings in (6), one

obtains the following spectral representation for the amplitude:

$$\mathscr{A}_\mu^j(q^2) = i \int_0^{+\infty} dE \, \frac{\rho(E)}{2E} \frac{\langle \pi^j(\mathbf{p})| \, J_\mu(0) \, |E, \mathbf{k}\rangle \, \langle E, \mathbf{k}| \, H_W(0) \, |K^j(\mathbf{k})\rangle}{E_K(\mathbf{k}) - E + i\varepsilon}$$
$$- i \int_0^{+\infty} dE \, \frac{\rho_S(E)}{2E} \frac{\langle \pi^j(\mathbf{p})| \, H_W(0) \, |E, \mathbf{p}\rangle \, \langle E, \mathbf{p}| \, J_\mu(0) \, |K^j(\mathbf{k})\rangle}{E - E_\pi(\mathbf{p}) + i\varepsilon} \,, \tag{11}$$

where ρ and ρ_S are the associated spectral densities. For what follows it is important to notice that ρ (ρ_S) selects only states with strangeness $S = 0$ ($S = 1$).

B. Euclidean correlators

For the remainder of the paper we assume that the vector current is the conserved one as given by Noether's theorem and which depends on the chosen lattice discretization of QCD. The rare kaon decay amplitudes will be determined by computing Euclidean correlation functions and we now turn to a discussion of these. Throughout this section we consider the time dimension to be infinite or very large compared to the time separations of the inserted operators.

1. 2-point functions

To obtain the energy of single-meson states we consider the following 2-point function:

$$\Gamma_P^{(2)}(t, \mathbf{p}) = \langle \phi_P(t, \mathbf{p}) \phi_P^\dagger(0, \mathbf{p})\rangle \,, \tag{12}$$

where $\phi_P(t, \mathbf{p})$ is an annihilation operator for a pseudoscalar meson P with spatial momentum $\mathbf{p}$ at time t. For $t \gg 0$ (and $t \ll T/2$, where T is the temporal extent of the lattice), $\Gamma_P^{(2)}(t, \mathbf{p})$ has the following behavior:

$$\Gamma_P^{(2)}(t, \mathbf{p}) = \frac{|Z_P|^2}{2E_P(\mathbf{p})} e^{-E_P(\mathbf{p})t} \,, \tag{13}$$

with $Z_P = \langle 0| \, \phi_P(0, \mathbf{0}) \, |P(E_P(\mathbf{p}), \mathbf{p})\rangle$ and $E_P(\mathbf{p}) = \sqrt{M_P^2 + \mathbf{p}^2}$. Depending on the choice of interpolating operator ϕ_P, Z_P may (and in general will) depend on the momentum $\mathbf{p}$ but we do not exhibit this dependence explicitly here and in the following.
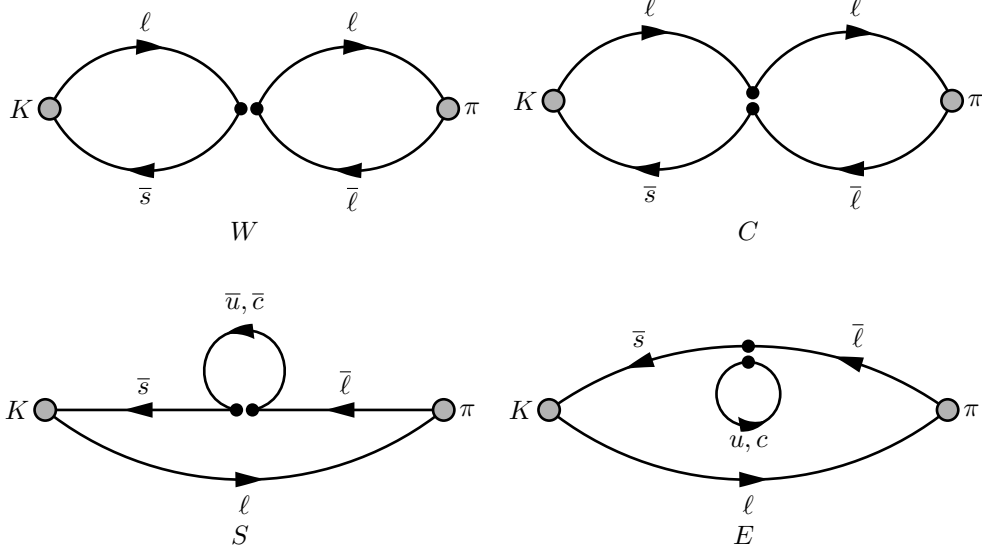
8

Figure 3. Diagrams contributing to the 3-point function $\Gamma_H^{(3)}(t_H, \mathbf{p})$ defined in Eq. (14). The two black circles represent the currents in the four-quark operators $Q_{1,2}^q$ defined in (8). ℓ denotes a light (u or d) quark propagator. The different topologies contain the operators Q_1^q or Q_2^q depending on whether the initial state is a charged or neutral kaon. For example, when the initial state is K^+, the W and S topologies contain an insertion of Q_2^q while the C and E topologies contain an insertion of Q_1^q.

2. 3-point functions

To obtain matrix elements of the effective weak Hamiltonian, we define the following 3-point function:

$$\Gamma_H^{(3)}(t_H, \mathbf{p}) = \int d^3\mathbf{x} \, \langle \phi_\pi(t_\pi, \mathbf{p}) H_W(t_H, \mathbf{x}) \phi_K^\dagger(0, \mathbf{p}) \rangle \tag{14}$$

with $0 < t_H < t_\pi$ and on a discrete lattice the integral over $\mathbf{x}$ is replaced by the corresponding sum. The 4 Wick contractions necessary to compute $\Gamma_H^{(3)}$ are illustrated in Fig. 3. For $0 \ll t_H \ll t_\pi$, $\Gamma_H^{(3)}$ has the following behavior:

$$\Gamma_H^{(3)}(t_H, \mathbf{p}) = \frac{Z_\pi Z_K^\dagger \mathcal{M}_H(\mathbf{p})}{4 E_\pi(\mathbf{p}) E_K(\mathbf{p})} e^{-E_\pi(\mathbf{p}) t_\pi} e^{-[E_K(\mathbf{p}) - E_\pi(\mathbf{p})] t_H} \,, \tag{15}$$

with $\mathcal{M}_H(\mathbf{p}) = \langle \pi(\mathbf{p}) | H_W(0) | K(\mathbf{p}) \rangle$. We also define the 3-point function of the electromagnetic current:

$$\Gamma_{J_\mu}^{(3)\,P_j}(t, t_J, \mathbf{p}, \mathbf{k}) = \int d^3\mathbf{x} \, e^{-i\mathbf{q}\cdot\mathbf{x}} \langle \phi_{P_j}(t, \mathbf{p}) J_\mu(t_J, \mathbf{x}) \phi_{P_j}^\dagger(0, \mathbf{k}) \rangle \,, \tag{16}$$

9

where P denotes the pseudoscalar meson ($P = \pi$ or K) and j its charge. This correlation function has the following asymptotic behavior for $t \gg t_J \gg 0$:

$$\Gamma^{(3)\,Pj}_{J_\mu}(t, t_J, \mathbf{p}, \mathbf{k}) = \frac{|Z_P|^2 \mathscr{M}^{Pj}_{J_\mu}(\mathbf{p}, \mathbf{k})}{4 E_{Pj}(\mathbf{p}) E_{Pj}(\mathbf{k})} e^{-(t-t_J)E_{Pj}(\mathbf{k})} e^{-t_J E_{Pj}(\mathbf{p})}, \tag{17}$$

where $\mathscr{M}^{Pj}_{J_\mu}(\mathbf{p}, \mathbf{k}) = \langle P^j(E_{Pj}(\mathbf{p}), \mathbf{p})| J_\mu(0) |P^j(E_{Pj}(\mathbf{k}), \mathbf{k})\rangle$ (note that $\mathscr{M}^{P0}_{J_0}(\mathbf{p}, \mathbf{p}) = 0$).

3. 4-point functions

In order to compute the amplitude (6), we define the following unintegrated 4-point correlation function:

$$\Gamma^{(4)\,j}_\mu(t_H, t_J, \mathbf{k}, \mathbf{p}) = \int \mathrm{d}^3\mathbf{x} \int \mathrm{d}^3\mathbf{y} \, e^{-i\mathbf{q}\cdot\mathbf{x}} \langle \phi_{\pi^j}(t_\pi, \mathbf{p}) \, \mathrm{T}[J_\mu(t_J, \mathbf{x}) H_W(t_H, \mathbf{y})] \, \phi^\dagger_{K^j}(0, \mathbf{k}) \rangle, \tag{18}$$

where $0 < t_J, t_H < t_\pi$. As explained in the next section, the rare kaon decay amplitudes are obtained by integrating $\Gamma^{(4)\,j}_\mu(t_H, t_J, \mathbf{k}, \mathbf{p})$ over t_H and t_J (or by exploiting time translation symmetry and integrating over their difference).

We now perform the quark Wick contractions in (18) to generate the diagrams which need to be evaluated. Assuming isospin symmetry in the quark masses, $m_u = m_d$, 20 types of diagrams have to be computed for the charged correlator and 2 additional ones are needed for the neutral correlator. We organize these diagrams in 5 classes, which are presented in Figs. 7–11. It is convenient to define the factor

$$Z_{K\pi}(t_\pi, \mathbf{k}, \mathbf{p}) = \frac{Z_\pi Z^\dagger_K}{4 E_\pi(\mathbf{p}) E_K(\mathbf{k})} e^{-E_\pi(\mathbf{p})t_\pi}, \tag{19}$$

which represents the propagation of the external pseudoscalar mesons in $\Gamma^{(4)\,j}_\mu(t_H, t_J, \mathbf{k}, \mathbf{p})$. This factor does not contribute to the rare kaon decay amplitude and we choose to define the normalized unintegrated correlator $\tilde{\Gamma}^{(4)\,j}_\mu \equiv \Gamma^{(4)\,j}_\mu / Z_{K\pi}$. The decay amplitudes are obtained by integrating $\tilde{\Gamma}^{(4)\,j}_\mu$ over t_H and t_J as explained in the following subsection. We note however, that if the times are sufficiently separated for $\tilde{\Gamma}^{(4)\,j}_\mu$ to be dominated by single particle intermediate states, then one has:

$$\tilde{\Gamma}^{(4)\,j}_\mu(t_H, t_J, \mathbf{k}, \mathbf{p}) = \begin{cases} \dfrac{\mathscr{M}_H(\mathbf{k})\mathscr{M}^{\pi^j}_{J_\mu}(\mathbf{p}, \mathbf{k})}{2 E_\pi(\mathbf{k})} e^{-E_K(\mathbf{k})t_H} e^{-E_\pi(\mathbf{k})(t_J - t_H)} e^{E_\pi(\mathbf{p})t_J} & \text{if} \quad 0 \ll t_H \ll t_J \\[4mm] \dfrac{\mathscr{M}_H(\mathbf{p})\mathscr{M}^{K^j}_{J_\mu}(\mathbf{p}, \mathbf{k})}{2 E_K(\mathbf{p})} e^{-E_K(\mathbf{k})t_J} e^{-E_K(\mathbf{p})(t_H - t_J)} e^{E_\pi(\mathbf{p})t_H} & \text{if} \quad t_J \ll t_H \ll t_\pi. \end{cases} \tag{20}$$

10

C. Extracting the rare kaon decay amplitude

In order to obtain the amplitude (6), we need to integrate the 4-point correlator $\tilde{\Gamma}_\mu^{(4)\,j}(t_H, t_J, \mathbf{k}, \mathbf{p})$, defining the integrated correlator by:

$$I_\mu^j(T_a, T_b, \mathbf{k}, \mathbf{p}) = e^{-[E_\pi(\mathbf{p}) - E_K(\mathbf{k})]t_J} \int_{t_J - T_a}^{t_J + T_b} dt_H \, \tilde{\Gamma}_\mu^{(4)\,j}(t_H, t_J, \mathbf{k}, \mathbf{p}), \tag{21}$$

where $T_a, T_b > 0$. For T_a, T_b such that $0 \ll t_J - T_a < t_J + T_b \ll t_\pi$, this integrated correlator has the following spectral representation:

$$
\begin{aligned}
I_\mu^j(T_a, T_b, \mathbf{k}, \mathbf{p}) = &-\int_0^{+\infty} dE \, \frac{\rho(E)}{2E} \frac{\langle \pi^j(\mathbf{p})| \, J_\mu(0) \, |E, \mathbf{k}\rangle \, \langle E, \mathbf{k}| \, H_W(0) \, |K^j(\mathbf{k})\rangle}{E_K(\mathbf{k}) - E} (1 - e^{[E_K(\mathbf{k}) - E]T_a}) \\
&+ \int_0^{+\infty} dE \, \frac{\rho_S(E)}{2E} \frac{\langle \pi^j(\mathbf{p})| \, H_W(0) \, |E, \mathbf{p}\rangle \, \langle E, \mathbf{p}| \, J_\mu(0) \, |K^j(\mathbf{k})\rangle}{E - E_\pi(\mathbf{p})} (1 - e^{-[E - E_\pi(\mathbf{p})]T_b}), \tag{22}
\end{aligned}
$$

where, as in Minkowski space in Eq. (11), ρ and ρ_S are the spectral densities of non-strange and strangeness $S = 1$ states respectively. In finite-volume, we write the spectral densities as $\rho(E) = \sum_n (2E_n)\delta(E - E_n)$ (and similarly for ρ_S) so that the integrals reduce to sums over the finite-volume states n. The exponential factor in Eq. (21) is introduced to cancel the t_J dependence in (22). To recover the Minkowski amplitude (6), one needs to consider the $T_a, T_b \to +\infty$ limit of $I_\mu^j(T_a, T_b, \mathbf{k}, \mathbf{p})$. Since ρ selects states with strangeness $S = 0$, the contribution of the states with $E < E_K(\mathbf{k})$ diverge exponentially as $T_a \to +\infty$ in the first integral of (22). This is a standard feature in the evaluation of long-distance contributions (see e.g. [21, 22] for a detailed discussion in the context of the K_L-K_S mass difference). These contributions must be subtracted in order to extract the rare kaon matrix element from Euclidean correlation functions. Note that there are no exponentially growing terms with T_b, since all the strange states with momentum $\mathbf{p}$ have energies larger than $E_\pi(\mathbf{p})$. We define the subtracted, integrated correlator $\overline{I}_\mu^j(T_a, T_b, \mathbf{k}, \mathbf{p})$ by subtracting all the terms which grow exponentially with T_a from the right-hand side of (22). With this definition we can write the rare kaon decay amplitude as follows:

$$\mathscr{A}_\mu^j(q^2) = -i \lim_{T_{a,b} \to \infty} \overline{I}_\mu^j(T_a, T_b, \mathbf{k}, \mathbf{p}). \tag{23}$$

How does one compute the subtracted quantity $\overline{I}_\mu^j(T_a, T_b, \mathbf{k}, \mathbf{p})$ in practice? For physical values of the quark masses, the only intermediate states that can generate an exponentially growing term in (22) are ones consisting of 1, 2 or 3 pions, the vacuum intermediate state being forbidden by parity conservation. We will now discuss each of these cases, providing two different approaches for the treatment of the dominant single-pion contribution.

11

1. Removal of the single-pion divergence, first method

The unphysical divergent term in (22) coming from the single pion intermediate state is given by:

$$D_\pi(T_a, \mathbf{k}, \mathbf{p}) = \frac{1}{2E_\pi(\mathbf{k})} \frac{\mathscr{M}_{J_\mu}^{\pi^j}(\mathbf{q})\mathscr{M}_H(\mathbf{k})}{E_K(\mathbf{k}) - E_\pi(\mathbf{k})} e^{[E_K(\mathbf{k}) - E_\pi(\mathbf{k})]T_a}, \tag{24}$$

where the notation of Sec. III B has been used. Because the pion is a stable state in QCD, $D_\pi(T_a, \mathbf{k}, \mathbf{p})$ can be entirely determined by fitting the asymptotic time behavior of the 2 and 3-point functions as described in Sec. III B.

2. Removal of the single-pion divergence, second method

We propose a second method to remove the single-pion divergence which is more "automatic" than the previous approach. This method is analogous to the procedure used in the calculation of the K_L-K_S mass difference in [22]. It is based on an additive shift of the weak Hamiltonian:

$$H'_W(x, \mathbf{k}) \equiv H_W(x) + c_s(\mathbf{k})\bar{s}(x)d(x), \tag{25}$$

where $c_s(\mathbf{k})$ is chosen such that:

$$\langle \pi^j(\mathbf{k})| H'_W(0, \mathbf{k}) |K^j(\mathbf{k})\rangle = 0. \tag{26}$$

By replacing H_W with H'_W the divergent contribution from the single-pion state (24) is cancelled. We now show that the transformation (25) does not affect the rare kaon decay amplitude. The scalar density appearing in (25) can be written as a total divergence using the following vector Ward identity (which is satisfied exactly on the lattice):

$$i(m_s - m_d)\bar{s}d = \partial_\mu V_\mu^{\bar{s}d}, \tag{27}$$

where $V_\mu^{\bar{s}d}$ is the $\bar{s}d$ flavor non-diagonal vector Noether (conserved) current. The relevant matrix elements of the scalar density can now be written as :

$$\langle \pi^j(\mathbf{p})| \bar{s}(x)d(x) |E, \mathbf{p}\rangle = i\frac{E - E_\pi(\mathbf{p})}{m_s - m_d} \langle \pi^j(\mathbf{p})| V_0^{\bar{s}d}(x) |E, \mathbf{p}\rangle \tag{28}$$

$$\langle E, \mathbf{k}| \bar{s}(x)d(x) |K^j(\mathbf{k})\rangle = i\frac{E_K(\mathbf{k}) - E}{m_s - m_d} \langle E, \mathbf{k}| V_0^{\bar{s}d}(x) |K^j(\mathbf{k})\rangle. \tag{29}$$
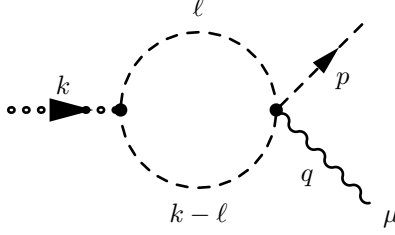
12

Figure 4. Two-pion intermediate state contribution to the rare kaon decay amplitude. The dotted and dashed lines represent respectively the kaon and pion propagators.

Using (22) and (23) we find that the total contribution of $c_s(\mathbf{k})\bar{s}d$ to the amplitude $\mathscr{A}_\mu^j(q^2)$ is proportional to:

$$\int \mathrm{d}^3\mathbf{x}\, e^{-i\mathbf{q}\cdot\mathbf{x}} \left\langle \pi^j(\mathbf{p}) \right| [J_\mu(t_J, \mathbf{x}), Q^{\bar{s}d}] \left| K^j(\mathbf{k}) \right\rangle = 0 \tag{30}$$

because of the vanishing commutator between the flavor-diagonal current J_μ and the flavor non-diagonal vector charge $Q^{\bar{s}d} = \int d^3\mathbf{y}\, V_0^{\bar{s}d}(t_H, \mathbf{y})$. Thus the physical amplitude is invariant under the transformation in Eq. (25). This property is independent of the value of $c_s(\mathbf{k})$ (and thus from the tuning condition (26)).

3. Removal of the two-pion divergence

In principle, a two pion intermediate state can contribute to a rare kaon decay through the process illustrated in Fig. 4. The matrix elements of vector and axial currents between a single-pion and a two-pion state have the following form factor decomposition:

$$\langle \pi(p_1) | V_\mu | \pi(p_2)\pi(p_3) \rangle = \varepsilon_{\mu\nu\rho\sigma} p_1^\nu p_2^\rho p_3^\sigma F(s, t, u) \tag{31}$$

where $s = (p_1 + p_2)^2$, $t = (p_1 - p_3)^2$ and $u = (p_2 - p_3)^2$.

We now show that the vector current does not contribute. Indeed, in Fig. 4 the $\pi\pi \to \pi\gamma^*$ vertex gives the following factor:

$$\varepsilon_{\mu\nu\rho\sigma} p^\nu k^\rho \int \frac{\mathrm{d}^4\ell}{(2\pi)^4} \frac{\ell^\sigma F(s, t, u)}{(\ell^2 + M_\pi^2)[(k - \ell)^2 + M_\pi^2]} . \tag{32}$$

Because of $O(4)$ invariance the integral in (32) can only be a linear combination of p^σ and k^σ which gives a vanishing contribution once contracted with the Levi-Civita symbol.

In the lattice theory, the cubic symmetry is sufficient for the integral (or the corresponding sum in a finite volume) to be a vector, but with corrections which vanish as the lattice spacing

13

$a \to 0$. At finite lattice spacing however, there is a non-zero two-pion contribution from lattice artifacts. For example, since the four-component quantity $\{(k_1)^3, (k_2)^3, (k_3)^3, (k_4)^3\}$ transforms as the same four-dimensional irreducible representation of the cubic group as k, one can imagine terms of the form $a^2 \varepsilon_{\mu\nu\rho\sigma} p^\nu k^\rho (k^\sigma)^3$ to be present. These terms will be amplified by the growing exponential factor in (22) and will need to be considered in the analysis. By studying the behavior with a^2 and T_a we anticipate being able to confirm our expectation that these effects are very small. For example, in our study of ΔM_K, the K_L-K_S mass difference [21, 22], with an inverse lattice spacing of $1.73\,\mathrm{GeV}$ and a pion mass of $330\,\mathrm{MeV}$, we find that the on-shell two-pion contributions are just a few per-cent and the artifacts are of $O(3\%)$ of these. Assuming similar factors here, the exponential factor $e^{[E_K(\mathbf{k})-E]T_a}$ in (22) would be insufficient for practical values of T_a to make the two-pion contribution significant until the calculations reach sub-percent precision.

4. Removal of the three-pion divergence

Contributions containing three-pion intermediate states are generated by diagrams such as those in Fig. 5. By comparing the measured widths of $K_S \to \pi\pi$ decays to those of $K_{S,+} \to \pi\pi\pi$ decays we estimate the relative phase-space suppression to be a factor of $O(1/500)$ or smaller. Moreover, as explained above, we already expect the on-shell two-pion contribution to be very small (of order a few percent) and so we anticipate that the on-shell three-pion contribution is negligibly small.

For the the diagram in Fig. 5(a) the contribution to the growing exponential in (22) can be avoided completely by restricting the calculations to $q^2 \leq 4M_\pi^2$, thus cutting out a small region of phase-space. This still allows us to determine the amplitudes in most of the q^2 range and to compare lattice results with ChPT-based phenomenological models and data where this is available. Although it is the diagram in Fig. 5(a) which is dominant in phenomenological analyses based on ChPT [17], the imaginary part, corresponding to the three-pion intermediate state, is neglected.The exponentially growing terms from diagrams such as Fig. 5(b) cannot be avoided in this way and we rely on the phase-space suppression described above. (Moreover, much of the exploratory work necessary to develop control of the different aspects of the procedure described in this paper, will be performed at heavier u and d quark masses, with the mass of the kaon below the three-pion threshold.)
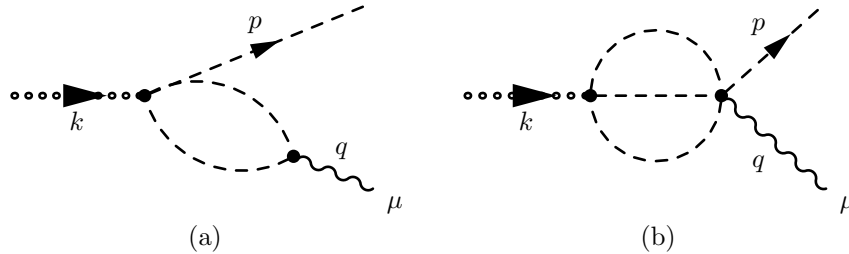
14

Figure 5. Examples of contributions from a three-pion intermediate state to rare kaon decays.

In the relatively distant future, if the precision required by experimental measurements and achievable in lattice computations is sufficiently high one can imagine, in principle at least, reconstructing the contributions from three-pion intermediate states explicitly as proposed in Sec. III C 1 and removing the associated exponential divergences in (22). Computing the relevant matrix elements is very challenging however, and the recently developed theory of trihadron states on a torus [23] is, so far at least, purely theoretical and has not been used in a practical lattice calculation. $K \to \pi\pi\pi$ matrix elements have also not been computed to date.

IV. FINITE VOLUME EFFECTS

In this section we briefly discuss issues concerning the finite-volume corrections arising from the evaluation of rare kaon decay amplitudes computed in a finite, periodic hypercubic lattice. The creation of on-shell intermediate multi-particle states will generate finite-volume corrections which decrease only as powers of the volume and not only exponentially. Thus in addition to generating exponentially growing terms in (22) (see the discussion in Sec. III C), power corrections are present if there are multi-hadron intermediate states with a smaller energy than M_K. We therefore have to identify the potential on-shell intermediate multi-particle states which can be created in rare kaons decays. This is similar to what was done in Sec. III C for the subtraction of unphysical divergences in the Euclidean amplitude. We have already shown in Sec. III C 3 that with a vector current there are no two-pion intermediate states and that for $q^2 < 4M_\pi^2$ there is no power correction from diagrams such Fig. 5(a). The arguments given in the preceding section that the remaining contributions from three-pion intermediate states are negligibly small applies here as well. Thus, at the levels of precision likely to be achievable in the near future, we do not have to correct for power-like

15

finite-volume effects.

There has been considerable work recently devoted to understanding the finite-volume corrections in three-hadron intermediate states [23]. If and when the precision of lattice computations of rare kaon decays amplitudes reaches the precision requiring the control of these effects, then it is to be hoped that the theoretical understanding provided in [23] can be developed into a practical technique generalizing the use of the Lellouch-Lüscher factor in $K \to \pi\pi$ decay amplitudes [24].

V. RENORMALIZATION

The ultraviolet divergences which appear in the evaluation of the matrix elements of the form $\int \mathrm{d}^4 x \, \langle f | \, \mathrm{T}[O_1(0)O_2(x)] \, |i\rangle$, where $O_{1,2}$ are local composite operators and $|i\rangle$, $|f\rangle$ represent the initial and final states, may come from two sources. Firstly $O_{1,2}$ themselves generally require renormalization and secondly additional divergences may appear as the two operators approach each other in the integral, i.e. as $x \to 0$. This is a general feature in the evaluation of long-distance contributions to physical processes. In the evaluation of the rare kaon decay amplitude (6) O_1 is the vector current and O_2 is the effective $\Delta S = 1$ Hamiltonian density and we start by briefly recalling the normalization of these operators before considering the contact terms arising as they approach each other.

A. Renormalization of H_W and J_μ

We assumed in Sec. III B that the current J_μ is the conserved one given by Noether's theorem applied to the chosen QCD action being used. It therefore satisfies the following vector Ward identity:

$$\partial_\mu \, \langle V_\mu^q(x) \, O(x_1, \ldots, x_n) \rangle = 0 \tag{33}$$

where $O(x_1, \ldots, x_n)$ is a multi-local operator with all the points $x_1, \ldots, x_n$ distinct from x. On the lattice, this identity is exactly satisfied and the derivative becomes a backward finite difference operator. This exact conservation means that the vector current does not require any renormalization as the continuum limit is taken.

The Wilson coefficients $C_{1,2}$ in the weak Hamiltonian H_W defined in (7) are currently known at NLO in the $\overline{\mathrm{MS}}$ scheme [10]. Since renormalization conditions based directly on
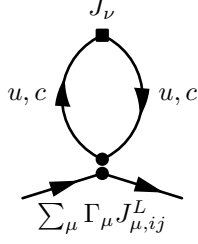
16

Figure 6. A potentially quadratically divergent insertion into the S and E classes of diagram. J_ν represents the conserved electromagnetic current and $J^L_{\mu,ij}$ is the local vector current $\bar{u}_j\gamma_\mu u_i$ or $\bar{c}_j\gamma_\mu c_i$ from $Q_{1,2}$.

dimensional regularization, such as the $\overline{\text{MS}}$ scheme, are purely perturbative we envisage following the standard practice of renormalizing the bare lattice operators $Q^u_1 - Q^c_1$ and $Q^u_2 - Q^c_2$ non-perturbatively into a scheme such as RI-MOM or RI-SMOM [25–27] and then to use continuum perturbation theory to match these renormalized operators into the $\overline{\text{MS}}$ scheme.

The use of a lattice formulation with good chiral symmetry, such as domain wall fermions, prevents mixing with dimension-6 operators which transform under different representations of the chiral flavor group $SU(4)_L \times SU(4)_R$. Within this formulation we can follow the renormalization procedure described in detail in [21, 22] in the evaluation of the K_L-K_S mass difference. In that case the effective weak Hamiltonian is a simple extension of (7),

$$H^{\Delta M_K}_W = \frac{G_F}{\sqrt{2}} \sum_{q,q'=u,c} V_{qd} V^*_{q's} \left(C_1 Q^{qq'}_1 + C_2 Q^{qq'}_2 \right) \tag{34}$$

where the operators are generalizations of those in Eq. (8)

$$Q^{qq'}_1 = (\bar{s}_i \gamma^L_\mu d_i)(\bar{q}_j \gamma^{L\,\mu} q'_j) \qquad \text{and} \qquad Q^{qq'}_2 = (\bar{s}_i \gamma^L_\mu d_j)(\bar{q}_j \gamma^{L\,\mu} q'_i). \tag{35}$$

Since the components with $q \neq q'$ do not contribute to the matrix elements for $K \to \pi\ell^+\ell^-$ decays, one is able to rewrite H_W in Eq. (34) in the form given in Eq. (7).

B. Additional divergences as $H_W(x)$ approaches $J(0)$

In diagrams of the "loop" class in topologies S and E (*cf.* Figs. 9 and 10), there are insertions of the form illustrated in Fig. 6. This has been studied in some detail in [1] and we briefly summarise the conclusions. The vector current J_ν to which the photon couples is

17

the conserved one whereas the vector current J_μ^L from the weak Hamiltonian is a local one; the label L represents *Local*. By power counting the loop integral appears to be quadratically divergent. This is reminiscent of the evaluation of the one-loop contribution to the vacuum polarization in QED and QCD and just as in those cases, electromagnetic gauge invariance implies that there is a transversality factor of $q^\mu q^\nu - q^2 g^{\mu\nu}$ and the order of divergence is reduced by two to a logarithmic one. (In momentum space with a lattice action the Ward identity $q^\nu J_\nu = 0$ becomes $\hat{q}^\nu J_\nu = 0$, with $\hat{q}^\nu \equiv (2/a)\sin(aq^\nu/2)$.) This structure was verified and the divergence explicitly calculated in [1] in one-loop lattice perturbation theory for Wilson, clover and twisted-mass fermions. The logarithmic divergence is mass independent, and so cancels exactly in the GIM subtraction between the diagrams with u and c-quark loops.

The above argument can be extended straightforwardly to higher-order diagrams in which the gluons are contained within the u or c quark loop in Fig. 6. The emission of one or more gluons from the u or c propagators in the loop to be absorbed by a quark or gluon propagator which is external to the loop reduces the order of divergence, again leading to a convergent loop integration as $J_\nu(x)$ approaches H_W. The remaining divergences are those which are associated with the renormalization of H_W.

We have seen that as a result of gauge invariance and the GIM mechanism in the four-flavor theory there are no additional UV divergences in $\int \mathrm{d}^4 x \, \langle \pi | \, T[J(0) \, H_W(x)] \, | K \rangle$ coming from the short distance region $x \simeq 0$. In the three-flavor theory, gauge invariance still protects the correlation function from quadratic divergences, but then there remains a logarithmic term which can be removed using non-perturbative renormalization techniques [25].

VI. CONCLUSIONS

Precision flavor physics will continue to be a central tool in searches for *new physics* and in guiding and constraining the construction of theories beyond the Standard Model. Lattice QCD simulations play an important rôle in quantifying the non-perturbative hadronic effects in weak processes. We must therefore continue to both improve the precision of the determination of standard quantities (such as leptonic decay constants, semileptonic form factors, neutral meson mixing amplitudes etc.) and to extend the range of physical quantities which become amenable to lattice simulations. In this paper we propose a procedure for the

evaluation of the long-distance effects in the rare kaon decay amplitudes $K \to \pi \ell^+ \ell^-$. These effects represent a significant (and unknown) fraction of the amplitudes. In a companion paper [2] we discuss the prospects for the evaluation of long distance contributions to the rare decays $K \to \pi \nu \bar{\nu}$ which will soon be measured by the NA-62 experiment at CERN and the KOTO experiment at J-PARC. These decays are dominated by short-distance contributions, but given that they will soon be measured, it is interesting also to determine the long-distance effects which are expected to be of the order of a few percent for K^+ decays.

In the previous sections we have explained how the technical issues needed to perform the lattice simulations can be resolved. Unphysical terms which grow exponentially with the range of the time integration, generally present when evaluating long-distance effects containing intermediate states with energies which are less than those of the external states, were shown in Sec. III C to be absent or small. They could potentially arise from the presence of intermediate states consisting of one, two or three pions and we considered each of these cases in turn. Similarly, the corresponding finite-volume corrections are small provided that the invariant mass of the lepton-pair is smaller than $2M_\pi$. Ultraviolet effects were discussed in Sec. V. We envisage using the lattice conserved electromagnetic vector current J_μ so no renormalization of this operator is required. In addition to the now standard renormalization of the weak Hamiltonian H_W, we need to consider the possible additional ultraviolet divergences which may arise when J_μ and H_W approach each other. Electromagnetic gauge invariance implies that no quadratic divergence is present [1] and in the four-flavor theory the remaining logarithmic divergence is cancelled by the GIM mechanism.

We conclude that it is now feasible to begin studying rare kaon decays $K \to \pi \ell^+ \ell^-$ in lattice simulations and in particular to computing the long-distance contributions. The next step is to figure out how to practically implement the numerical calculation of these amplitudes. The main challenge resides in the calculation of the 4-point function in Eq. (18). One important problem is the evaluation of diagrams containing closed loops which require the knowledge of quark propagators from a point to itself for every lattice site. Actual numerical calculations have been underway for the past two years [28] and we are preparing papers describing exploratory results. Within the next five years we would hope that the hadronic effects in these decays would be quantified with good precision, thus motivating the extension of the experimental studies of $K \to \pi \nu \bar{\nu}$ decays to include also $K \to \pi \ell^+ \ell^-$ decays.
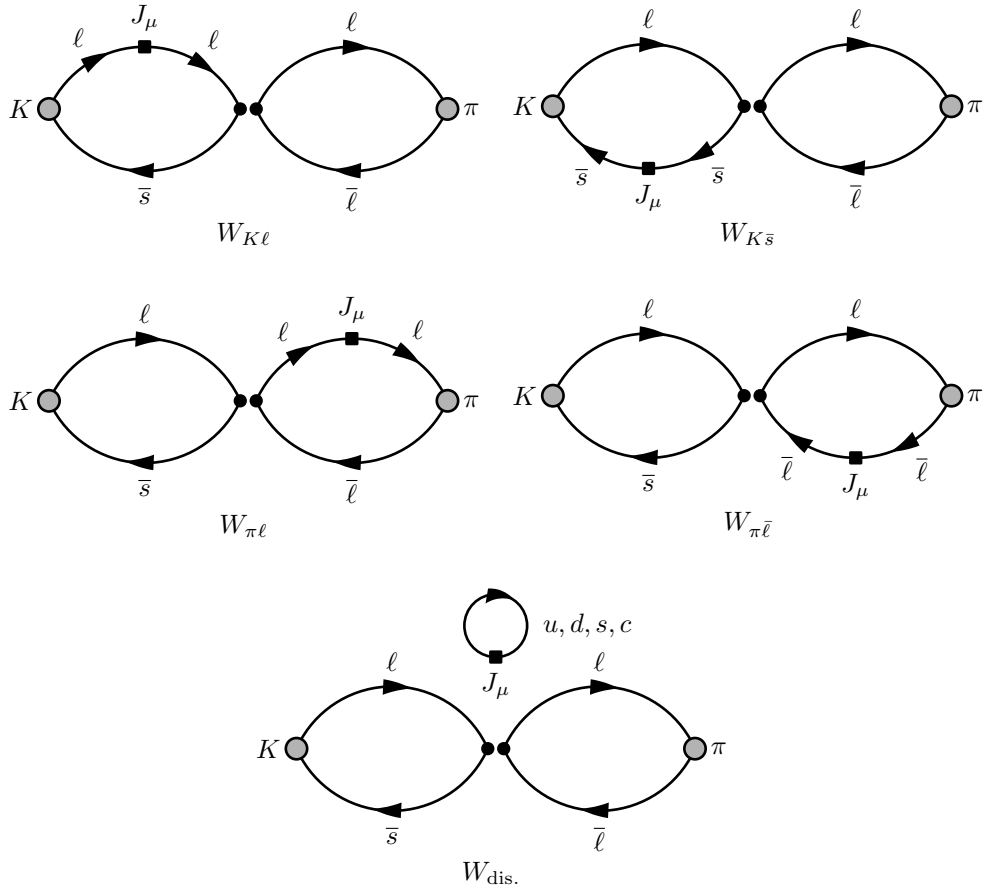
ACKNOWLEDGMENTS

Figure 7. "Wing" class of diagram contributing to the rare kaon decay correlator (18). The diagrammatic conventions are the same as those in Fig. 3.
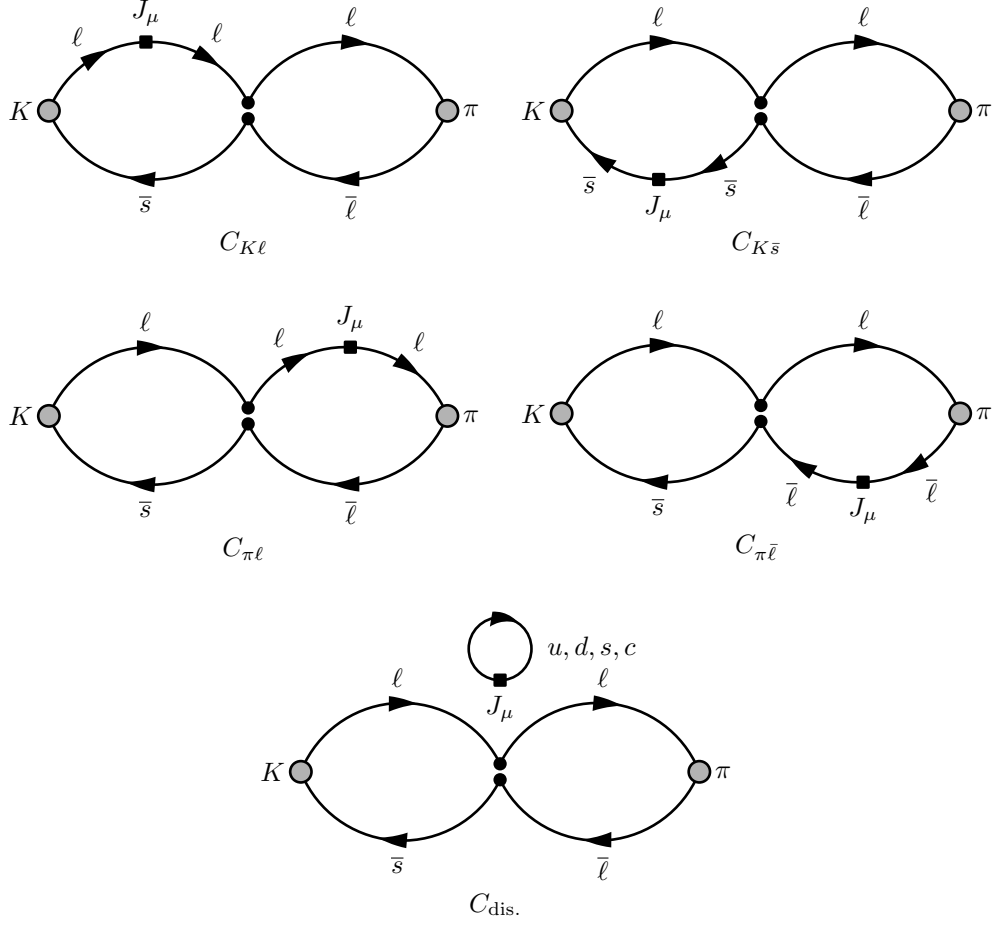
Figure 8. "Connected" class of diagram contributing to the rare kaon decay correlator (18). The diagrammatic conventions are the same as those in Fig. 3.The ℓ quark is an up or down quark depending on the charge of the initial and final states.
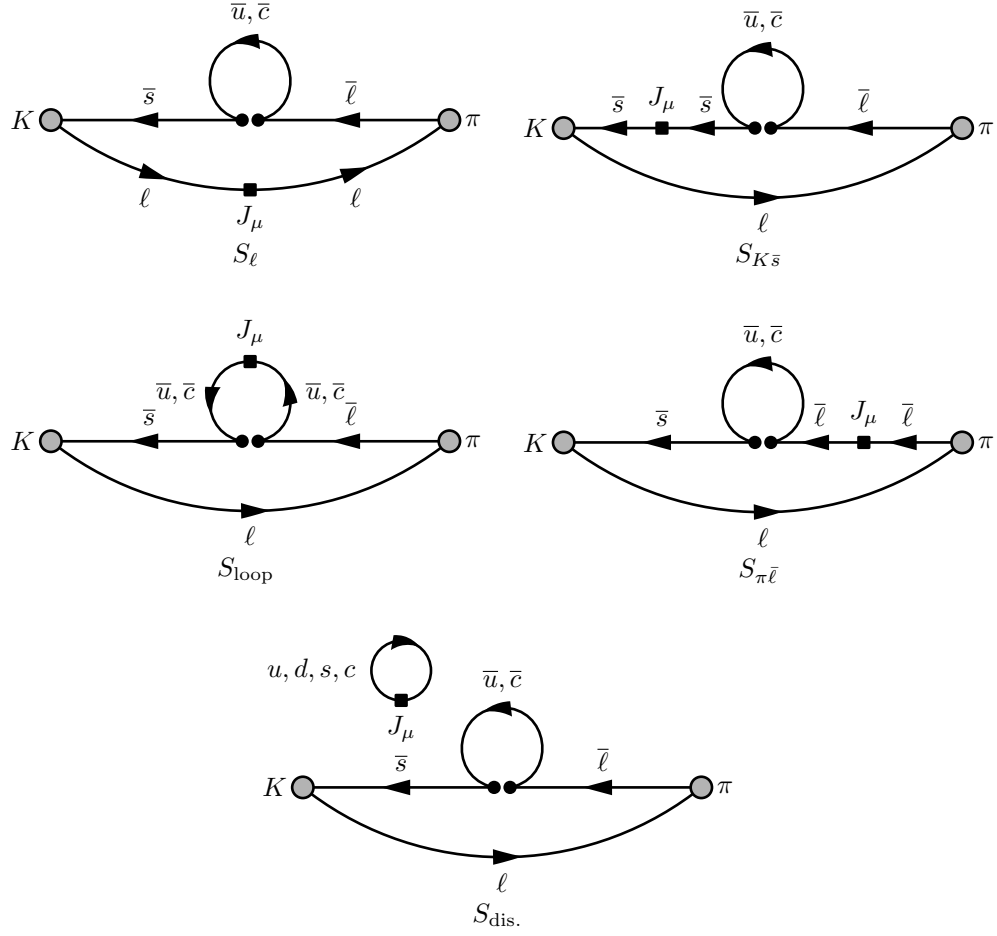
Figure 9. "Saucer" class of diagram contributing to the rare kaon decay correlator (18). The diagrammatic conventions are the same as those in Fig. 3.
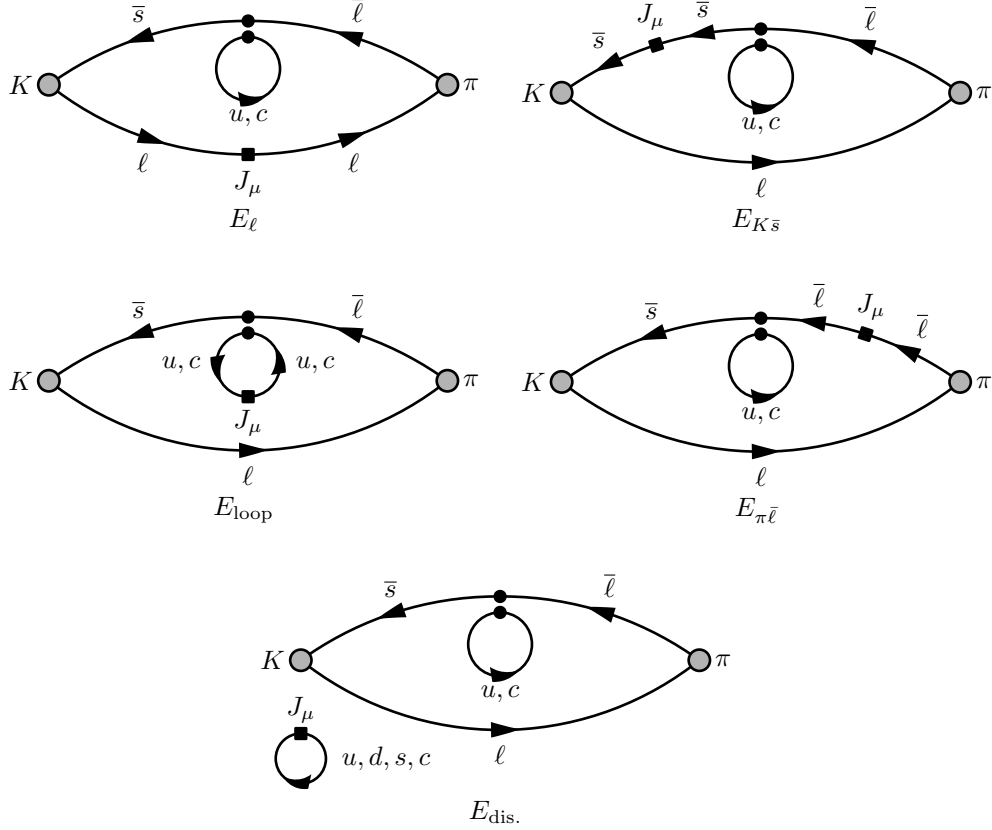
Figure 10. "Eye" class of diagram contributing to the rare kaon decay correlator (18). The diagrammatic conventions are the same as those in Fig. 3.
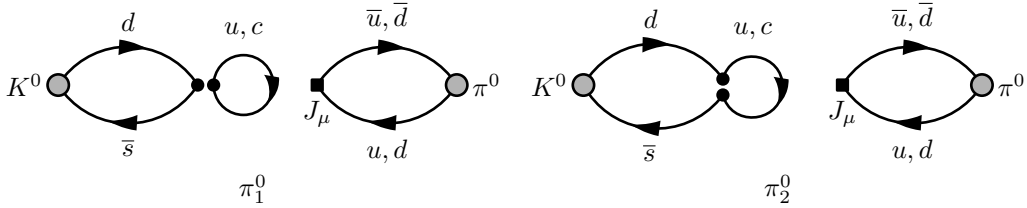

Figure 11. "π^0" class of diagram contributing to the rare kaon decay correlator (18). These diagrams only contribute to the decay of the neutral meson K^0. The diagrammatic conventions are the same as those in Fig. 3.

[1] G. Isidori, G. Martinelli, and P. Turchetti, Phys.Lett. **B633**, 75 (2006), arXiv:hep-lat/0506026 [hep-lat].

[2] N. Christ, X. Feng, A. Portelli, and C. Sachrajda (RBC-UKQCD), in preparation (2015).

[3] P. Bloch, S. Brehin, G. Bunce, B. Bloch-Devaux, A. Diamant-Berger, *et al.* (RBC-UKQCD), Phys.Lett. **B56**, 201 (1975).

[4] J. Batley *et al.* (NA48/2 Collaboration), Phys.Lett. **B677**, 246 (2009), arXiv:0903.3130 [hep-ex].

[5] J. Batley *et al.* (NA48/2 collaboration), Phys.Lett. **B697**, 107 (2011), arXiv:1011.4817 [hep-ex].

[6] J. Batley *et al.* (NA48/1 Collaboration), Phys.Lett. **B576**, 43 (2003), arXiv:hep-ex/0309075 [hep-ex].

[7] J. Batley *et al.* (NA48/1 Collaboration), Phys.Lett. **B599**, 197 (2004), arXiv:hep-ex/0409011 [hep-ex].

[8] A. Alavi-Harati *et al.* (KTeV Collaboration), Phys.Rev.Lett. **93**, 021805 (2004), arXiv:hep-ex/0309072 [hep-ex].

[9] A. Alavi-Harati *et al.* (KTEV Collaboration), Phys.Rev.Lett. **84**, 5279 (2000), arXiv:hep-ex/0001006 [hep-ex].

[10] G. Buchalla, A. J. Buras, and M. E. Lautenbacher, Rev.Mod.Phys. **68**, 1125 (1996), arXiv:hep-ph/9512380 [hep-ph].

[11] G. D'Ambrosio and G. Isidori, Int.J.Mod.Phys. **A13**, 1 (1998), arXiv:hep-ph/9611284 [hep-ph].

[12] P. Buchholz and B. Renk, Prog.Part.Nucl.Phys. **39**, 253 (1997).

[13] A. J. Buras and R. Fleischer, Adv.Ser.Direct.High Energy Phys. **15**, 65 (1998), arXiv:hep-ph/9704376 [hep-ph].

[14] A. Barker and S. H. Kettell, Ann.Rev.Nucl.Part.Sci. **50**, 249 (2000), arXiv:hep-ex/0009024 [hep-ex].

[15] V. Cirigliano, G. Ecker, H. Neufeld, A. Pich, and J. Portoles, Rev.Mod.Phys. **84**, 399 (2012), arXiv:1107.6001 [hep-ph].

[16] C. O. Dib, I. Dunietz, and F. J. Gilman, Phys.Rev. **D39**, 2639 (1989).

[17] G. D'Ambrosio, G. Ecker, G. Isidori, and J. Portoles, JHEP **9808**, 004 (1998), arXiv:hep-ph/9808289 [hep-ph].

[18] G. Isidori, C. Smith, and R. Unterdorfer, Eur.Phys.J. **C36**, 57 (2004), arXiv:hep-ph/0404127 [hep-ph].

[19] F. Mescia, C. Smith, and S. Trine, JHEP **0608**, 088 (2006), arXiv:hep-ph/0606081 [hep-ph].

[20] G. Ecker, A. Pich, and E. de Rafael, Nucl.Phys. **B291**, 692 (1987).

[21] N. H. Christ, T. Izubuchi, C. T. Sachrajda, A. Soni, and J. Yu (RBC-UKQCD), Phys.Rev. **D88**, 014508 (2013), arXiv:1212.5931 [hep-lat].

[22] Z. Bai, N. Christ, T. Izubuchi, C. Sachrajda, A. Soni, *et al.*, Phys.Rev.Lett. **113**, 112003 (2014), arXiv:1406.0916 [hep-lat].

[23] M. T. Hansen and S. R. Sharpe, (2014), arXiv:1408.5933 [hep-lat].

[24] L. Lellouch and M. Luscher, Commun.Math.Phys. **219**, 31 (2001), arXiv:hep-lat/0003023 [hep-lat].

[25] G. Martinelli, C. Pittori, C. T. Sachrajda, M. Testa, and A. Vladikas, Nucl.Phys. **B445**, 81 (1995), arXiv:hep-lat/9411010 [hep-lat].

[26] C. Sturm, Y. Aoki, N. Christ, T. Izubuchi, C. Sachrajda, *et al.*, Phys.Rev. **D80**, 014501 (2009), arXiv:0901.2599 [hep-ph].

[27] Y. Aoki, R. Arthur, T. Blum, P. Boyle, D. Brommel, *et al.*, Phys.Rev. **D84**, 014503 (2011), arXiv:1012.4178 [hep-lat].

[28] A. Lawson *et al.* (RBC-UKQCD), in *33rd International Symposium on Lattice Field Theory (Lattice 2015) Kobe, Japan, July 14-18, 2015* (2015).